Temperature dependence of the Urbach optical absorption edge: A theory of multiple phonon absorption and emission sidebands

C. H. Grein and Sajeev John

Joseph Henry Laboratories of Physics, Jadwin Hall, Princeton University, P.O. Box 708, Princeton, New Jersey 08544

(Received 11 July 1988)

The optical absorption coefficient for subgap electronic transitions in crystalline and disordered semiconductors is calculated by first-principles means with use of a variational principle based on the Feynman path-integral representation of the transition amplitude. This incorporates the synergetic interplay of static disorder and the nonadiabatic quantum dynamics of the coupled electron-phonon system. Over photon-energy ranges of experimental interest, this method predicts accurate linear exponential Urbach behavior of the absorption coefficient. At finite temperatures the non-linear electron-phonon interaction gives rise to multiple phonon emission and absorption sidebands which accompany the optically induced electronic transition. These sidebands dominate the absorption in the Urbach regime and account for the temperature dependence of the Urbach slope and energy gap. The physical picture which emerges is that the phonons absorbed from the heat bath are then reemitted into a dynamical polaronlike potential well which localizes the electron. At zero temperature we recover the usual polaron theory. At high temperatures the calculated tail is qualitatively similar to that of a static Gaussian random potential. This leads to a linear relationship between the Urbach slope and the downshift of the extrapolated continuum band edge as well as a temperature-independent Urbach focus. At very low temperatures, deviations from these rules are predicted arising from the true quantum dynamics of the lattice. Excellent agreement is found with experimental data on c-Si, a-Si:H, a-As$_2$Se$_3$, and a-As$_2$S$_3$. Results are compared with a simple physical argument based on the most-probable–potential-well method.

I. INTRODUCTION

A nearly universally observed feature of optical absorption spectra near band edges in crystalline and amorphous semiconductors is the Urbach-Martienssen absorption edge.[1] The absorption coefficient for optically induced electronic transitions from the valence- to the conduction-band tails obeys the rule

$$\alpha(v) = \alpha_0 \exp\{ [hv - E_G(T)]/E_0(T) \} , \qquad (1.1)$$

where hv is the photon energy and E_G and E_0 are temperature-dependent fitting parameters. Here, E_G is comparable to the band-gap energy and the Urbach slope E_0 is typically in the range 10–100 meV for amorphous semiconductors. This linear exponential behavior of the absorption coefficient may extend over ranges of photon energies up to ~ 0.5 eV wide corresponding to as many as five decades in $\alpha(v)$.

Many theories of band-tail absorption consider a simple model of an electron interacting with spatially random, static potentials which describe impurities in doped semiconductors or structural disorder in amorphous semiconductors.[2–8] This picture works well for heavily doped or amorphous semiconductors. However, in many materials the interaction between the electron and the dynamical quantum field of phonons gives rise to polaronic effects and a significant increase in the conduction- and valence-band-tail density of states (DOS).[9–15] Even in the absence of static disorder, for electron-phonon coupling above the small-polaron threshold, the many-body

DOS (electron and lattice) when projected onto the phonon vacuum exhibits an exponential tail below the one-electron continuum which terminates at the small-polaron ground state.[16] Such a projected DOS is relevant to optical absorption experiments which occur on a time scale short compared with that of lattice motion. In fact, we show in this paper that the optical absorption coefficient $\alpha(v)$ reduces precisely to such a projected DOS in the zero-temperature limit as the phonon absorption sidebands are turned off. Physically such polaronic band-tail states arise from local lattice fluctuations which oscillate slowly on the time scale required for the electron to oscillate within the potential well and thereby stabilize it.

In many real materials the electron–acoustic-phonon coupling is below the small-polaron threshold. However, with the addition of static disorder, polaronic potential wells can play an important role in the band tail. Because static potential fluctuations provide nucleation centers for small-polaron formation, a substantial synergetic interplay between static localization and polaron formation may occur at zero temperature even when the electron-phonon coupling is below the threshold for small-polaron formation in the crystal[15] (see Fig. 1). At finite temperatures, the nonlinear electron-phonon interaction results in the creation of multiple phonon emission and absorption sidebands in the optical absorption spectrum. These sidebands account for some of the main features of absorption spectra in the Urbach regime, such as the temperature independence of the Urbach focus and the temperature dependence of E_0 and E_G (see Figs. 2–6).
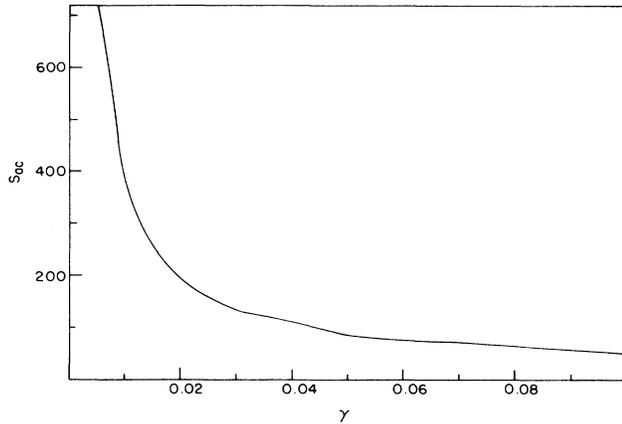
FIG. 1. Theoretical small-polaron "phase" diagram. In the absence of static disorder and at zero temperature, small-polaron formation can take place if the point (γ, S_{ac}) is above the line. S_{ac} is the electron–acoustic-phonon coupling constant and γ is the nonadiabaticity parameter.

We develop an expression for the optical absorption coefficient based on first principles. Both electron–acoustic-phonon and electron–static-disorder interactions are considered. A continuum effective-mass approximation is made for the electron dynamics. Due to the comparatively large static dielectric constants of Si, As_2Se_3, and As_2S_3, final-state interactions between electrons and holes are neglected. In these materials, the exciton binding energy is small compared with the energy scale of the disorder resulting in the exciton line appearing above the conduction-band-tail Urbach regime.

Good agreement is found between theoretical predictions and experimental measurements of the temperature dependence of the absorption coefficient of c-Si, a-Si:H, a-As_2Se_3, and a-As_2S_3. The physical parameters entering into the theory, the conduction- and valence-electron effective masses and electron-phonon deformation potentials, the Debye energy, the speed of sound (assuming linear dispersion for acoustic phonons), and the atomic masses were determined where possible from experimental measurements. For these and other unmeasured but physically reasonable values of the input parameters the theory reproduces the observed linear relationship between E_0 and E_G and the temperature independence of the Urbach focus.

The Feynman path-integral technique is used to obtain the one-electron propagator. This method was originally developed by Feynman[10] to obtain the ground-state energy of the Fröhlich Hamiltonian describing an electron interacting with optical phonons. The path integral over the electron coordinate is approximated by a first cumulant expansion about a trial action which describes an electron coupled to a single fictitious mass M_{trial} representing the phonon cloud by means of a spring with stiffness K_{trial}. Both M_{trial} and K_{trial} are variational parameters optimized according to a variational principle.[15] The adiabatic limit of the electron-phonon interaction is obtained by choosing $M_{\text{trial}} = \infty$.

The basic physical picture which emerges from our analysis is that the Urbach edge in crystals at finite temperatures can be quantitatively described by an optically induced electronic transition which is accompanied by multiple phonon absorptions from the heat bath.[17] These phonons are then reemitted into a polaronic potential well which then localizes the electron in the band tail. In the continuum model, this process by itself gives rise to an infinite exponentially decaying absorption tail since the elastic energy of lattice deformation is provided by the heat bath. In the case of disordered semiconductors, we find that this process significantly alters the spectrum of electronic states localized by static random potential wells and accounts for the observed temperature dependent aspects of Urbach's rule.

Section II outlines the effects of phonon sidebands on optical absorption spectra and includes a derivation of an expression for the optical absorption coefficient. In Sec. III the path-integral method is employed to obtain the absorption coefficient and a comparison is made with experimental measurements for several different materials. We find that good agreement with many aspects of the observed absorption edge may be obtained in a simple model of an electron initially in a single strongly localized state which is then optically excited into a band tail. In Sec. IV we present an argument that the corrections to this model arising from two band tails should be small. Section V contains a comparison of the results of Sec. III with the predictions of a simple physical argument. Results are discussed in Sec. VI.

II. PHONON SIDEBANDS AND THE OPTICAL ABSORPTION COEFFICIENT

At finite temperatures, optically induced electronic transitions are accompanied by multiple phonon absorption and emission sidebands. This sections begins with a definition and a simple example of sidebands and contains a development of an expression for the optical absorption coefficient in a one-electron approximation.

A sideband in an absorption spectrum is the excitation of an oscillator not subject to an external force simultaneously with the excitation of another oscillator which is subject to an external force. The former oscillator is excited through nonlinear interactions with the latter. Consider the following simple example:[18] two simple harmonic oscillators with coordinates x and y and frequencies ω_1 and ω_2 interact through a weak potential $\gamma \omega_1^2 x^2 y / 2$. Here x might represent an electron coordinate and y corresponds to a particular phonon. The classical equations of motion for this system are

$$\ddot{x} + \omega_1^2 x + \gamma \omega_1^2 x y = 0 , \tag{2.1a}$$

$$\ddot{y} + \omega_2^2 y + \frac{\gamma}{2} \omega_1^2 x^2 = 0 . \tag{2.1b}$$

In the absence of interaction, the solutions are

$$x = x_0 \exp(\pm i \omega_1 t) , \tag{2.2a}$$

$$y = y_0 \exp(\pm i \omega_2 t) . \tag{2.2b}$$

Substituting (2.2a) and (2.2b) into the final term in (2.1a) and solving for x produces a solution with sidebands of frequency $|\omega_1 \pm \omega_2|$ in addition to the principle frequency ω_1. Repeatedly substituting approximate solutions produces successive sideband terms with frequencies $|\omega_1 \pm n\omega_2|$ for all integers n.

We now consider a model for the optical absorption spectrum due to subgap transitions in an amorphous semiconductor. An electron may interact with both acoustic phonons and static random potentials. For this system the Hamiltonian is [15]

$$H = H_e + H_{ac} + H_{e\text{-}ac} + H_{dis} , \tag{2.3a}$$

where

$$H_e = p^2/2m^* \tag{2.3b}$$

is the kinetic energy of an electron of band mass m^*,

$$H_{ac} = \frac{M}{2} \sum_k (|\dot{q}_k|^2 + \omega_k^2 |q_k|^2) \tag{2.3c}$$

is the harmonic phonon energy for a lattice of N atoms of mass M,

$$H_{e\text{-}ac} = \frac{E_d}{u} \sum_k \dot{q}_k \frac{e^{i k \cdot x}}{\sqrt{N}} \tag{2.3d}$$

is the deformation potential interaction between the electron and the phonons, and

$$H_{dis} = \sum_{i=1}^{N_d} v(x - R_j) \tag{2.3e}$$

is a sum over N_d static potentials located at $\{R_j\}$. The wave-vector summations in (2.3c) and (2.3d) extend over all points in the first Brillouin zone. The normal coordinate of a longitudinal-acoustic phonon of wave vector k and frequency $\omega_k = uk$ is $q_k = \hat{k} \cdot q_k$, where u is the speed of sound. E_d is the deformation potential energy constant and following Sumi and Toyozawa[12] we define a dimensionless acoustic coupling constant S_{ac} through $\hbar u k_0 S_{ac} \equiv E_d^2/2Mu^2$ where $k_0 = \pi/a$ and a is the lattice spacing. The nonadiabaticity of the electron-phonon interaction is measured by $\gamma \equiv \hbar u k_0/(\hbar k_0^2/2m^*)$. A continuum theory may be obtained by replacing the wave vector summations by the weighted integral

$$\sum_k \rightarrow \frac{V}{(2\pi)^3} \int d^3k \, H_c(k) , \tag{2.4}$$

where V is the volume of the solid. We follow John and Cohen[14] in considering a cubic Brillouin zone with sides of length $2\pi/a$ and H_c defined by

$$H_c(k) = \exp\left[-\frac{\pi}{4} \left[\frac{k}{k_0} \right]^2 \right] \tag{2.5}$$

which preserves the volume of the first Brillouin zone. Term (2.3d) is the nonlinear interaction between the electron and acoustic phonons which will result in the optical absorption spectrum displaying phonon sidebands when the electron is excited by a photon.

Within a one-electron approximation the imaginary part of the dielectric constant as a function of photon energy $h\nu$ is[19]

$$\varepsilon_2(\nu) = (2\pi e)^2 \frac{2}{V} Av_i \left\{ \sum_f |R_{i,f}|^2 \delta(h\nu + E_i - E_f) \right\} , \tag{2.6}$$

where V is the illuminated volume of the sample, assumed to be the entire sample volume. The sum is over the final states of energy E_f and $Av_i\{\cdots\}$ denotes a thermal average over the initial states with energy E_i. The dipole matrix element takes the form

$$R_{i,f} = \langle \psi_f | \tau \cdot x | \psi_i \rangle , \tag{2.7}$$

where τ is the polarization vector of the photon and x is the electron position. In generalizing this one-electron expression to the many-body dynamics of a coupled electron-phonon system, the dipole matrix element is interpreted in an adiabatic approximation by factoring the many-body wave function into a product of a lattice wave function, and an electronic wave function $\psi_{i,f}(x)$.

Using the relation $\alpha(\nu) = \nu \varepsilon_2(\nu)/cn$,[19] where n is the real part of the refractive index, and dropping all constant prefactors and quantities which depend on photon energy more weakly than exponentially, the exponential part of the absorption coefficient becomes

$$\alpha(\nu) \sim Av_i \left\{ \sum_f |R_{i,f}|^2 \delta(E_i + h\nu - E_f) \right\}$$

$$= Av_i \left\{ \sum_f |R_{i,f}|^2 \int_{-\infty}^{\infty} \frac{dt}{2\pi\hbar} e^{it(E_i/\hbar + \nu - E_f/\hbar)} \right\}$$

$$= \int_{-\infty}^{\infty} \frac{dt}{2\pi\hbar} \sum_{i,f} |R_{i,f}|^2 e^{-\beta E_i}$$

$$\times e^{it(E_i/\hbar + \nu - E_f/\hbar)} \Bigg/ \left[\sum_i e^{-\beta E_i} \right] , \tag{2.8}$$

where $\beta = 1/k_B T$.

In some amorphous semiconductors, such as a-Si:H,[19] the absorption is dominated by a single band tail. For concreteness we will consider a simple model where the absorption is dominated by the conduction-band tail. The results can, nevertheless, be carried over to the case of an absorption edge dominated by a valence-band tail. In this model, the initial-state manifold consists of a single strongly localized level corresponding to an infinite hole effective mass. The electron does not interact with phonons, thus no valence-band tail forms in this approximation. In the final state, after the electronic transition, the electron interacts with both phonons and static potential fluctuations [described by Hamiltonian (2.3a)] resulting in the formation of a conduction-band tail in the DOS.

The continuum model we are employing does not allow for real band structure. It should, however, give a good description of subgap electronic transitions provided the tail does not extend more than one-quarter of the way into the gap and the localization lengths for the band-tail states are greater than or equal to the lattice constant. We define an energy scale where $-E_{gap}$ is the energy of

an electron in its initial localized state and on which zero represents the energy of an electron at rest in the conduction band in a phonon vacuum. Conduction-band-tail states may be referenced by the energy E (<0) defined by $h\nu - E_{gap} = E$.

Expression (2.8) describes the optical absorption when an electronic transition is induced from an initial localized state to a final state at energy E in the conduction-band tail. As is described in the next section, for physically reasonable choices of the electron-phonon coupling strength and nonadiabaticity, and mean static potential strength and correlation length, many properties of the absorption spectra calculated from (2.8) agree well with observed results for c-Si, a-Si:H, a-As$_2$S$_3$, and a-As$_2$Se$_3$.

III. PATH-INTEGRAL CALCULATION OF ABSORPTION COEFFICIENT AND RESULTS

This section describes the calculation of the absorption coefficient with the incorporation of the full nonadiabatic dynamics of the many-body electron-phonon system. Comparison with experimental results are also made.

To incorporate the nonadiabatic quantum dynamics of

the electron-phonon system, the absorption coefficient (2.8) is rewritten in terms of matrix elements of time evolution operators:[15]

$$\alpha(\nu) \sim \int_{-\infty}^{\infty} \frac{dt}{2\pi\hbar} e^{i(\nu - E_{gap}/\hbar)t}$$
$$\times \sum_{i,f} \langle i | e^{-(\beta - it/\hbar)H_{ac}} R | f \rangle$$
$$\times \langle f | e^{-itH/\hbar} R | i \rangle / Z , \qquad (3.1a)$$

where

$$Z \equiv \sum_i \langle i | e^{-\beta H_{ac}} | i \rangle . \qquad (3.1b)$$

Our model describes the optically induced electronic transition from an initial localized state at, say, the origin to localized states in the conduction-band tail. Since the model does not include electron-hole correlations, the main effect of R is to restrict the final-state electron coordinate to $\mathbf{x}=0$. Neglecting all dependence of $R_{i,f}$ on f allows one to factor it out of the summation in (3.1a). Writing the state vectors in a coordinate-space representation $|\mathbf{x};\{q_k\}\rangle$ results in (3.1a) becoming

$$\alpha(\nu) \sim \int_{-\infty}^{\infty} \frac{dt}{2\pi\hbar} e^{it(\nu - E_{gap})/\hbar} \int \prod_k (dq_k \, dq_k') \langle \{q_k\} | e^{-(\beta - it/\hbar)H_{ac}} | \{q_k'\} \rangle \langle 0; \{q_k'\} | e^{-iHt/\hbar} | 0; \{q_k\} \rangle . \qquad (3.2)$$

The first matrix element is that of a free harmonic oscillator and may be evaluated exactly. The second matrix element involving the full Hamiltonian H may be represented by the path integrals

$$\langle 0; \{q_k'\} | e^{-iHt/\hbar} | 0; \{q_k\} \rangle = \int \mathcal{D}\mathbf{x}(\tau) \mathcal{D}q_k(\tau) e^{iS/\hbar} \qquad (3.3)$$

with limits $\mathbf{x}(0)=\mathbf{x}(t)=0$ and $q_k(0)=q'_k, q_k(t)=q_k$ and where S is the action corresponding to the full Hamiltonian H. A straightforward but tedious calculation outlined in the Appendix yields

$$\int \prod_k (dq_k \, dq_k') \langle \{q_k\} | e^{-(\beta - it/\hbar)H_{ac}} | \{q_k'\} \rangle \langle 0; \{q_k'\} | e^{-iHt/\hbar} | 0; \{q_k\} \rangle = \int_{\mathbf{x}(0)=\mathbf{x}(t)=0} \mathcal{D}\mathbf{x}(\tau) e^{i\hbar^{-1}S_{eff}} \qquad (3.4)$$

where

$$S_{eff} = S_e + S_{int} + S_{dis} , \qquad (3.5a)$$

$$S_e = \frac{m^*}{2} \int_0^t \dot{\mathbf{x}}^2(\tau) d\tau ,$$

$$S_{int} = \int_0^t d\tau \int_0^t d\tau' \frac{1}{N} \sum_k e^{i\mathbf{k}\cdot[\mathbf{x}(\tau)-\mathbf{x}(\tau')]} \frac{\hbar u k_0}{2} S_{ac} i\omega_k$$

$$\times \{[N(\omega_k)+1] e^{-i\omega_k|\tau-\tau'|}$$

$$+ N(\omega_k) e^{i\omega_k\tau-\tau'|}\} , \qquad (3.5b)$$

and

$$S_{dis} = \frac{i}{2\hbar} \int_0^t d\tau \int_0^t d\tau' B[\mathbf{x}(\tau)-\mathbf{x}(\tau')] \qquad (3.5c)$$

with $N(\omega_k) \equiv (e^{\beta\hbar\omega_k}-1)^{-1}$ being the phonon occupation number. Term (3.5c) is obtained by averaging over all configurations of the static potentials and taking the limits of high density ($N_d/V \to \infty$) and weak scattering

($v \to 0$) with $N_d v^2/V$ remaining constant. B is the autocorrelation function of the static potentials,

$$B(\mathbf{x}(\tau)-\mathbf{x}(\tau')) \equiv \frac{N_d}{V} \int d\mathbf{R} \, v(\mathbf{x}(\tau)-\mathbf{R}) v(\mathbf{x}(\tau')-\mathbf{R}) . \qquad (3.6)$$

The average potential has been chosen to be zero,

$$\int d\mathbf{R} \, v(\mathbf{x}(\tau)-\mathbf{R}) = 0 . \qquad (3.7)$$

We consider Gaussian correlated random potentials

$$B(\mathbf{x}(\tau)-\mathbf{x}(\tau')) = V_{rms}^2 \exp\left[-\frac{|\mathbf{x}(\tau)-\mathbf{x}(\tau')|^2}{L^2}\right] \qquad (3.8)$$

correlated over distances L comparable to the interatomic spacing.[8]

The electron coordinate does not appear quadratically in (3.5) so path integral (3.4) cannot be done exactly. It is approximated by a first cumulant expansion about a trial action which describes an electron coupled to a mass through a spring,[14,20] as described in Sec. I. The trial action is

$$S_{\text{trial}} = \frac{m^*}{2} \int_0^t d\tau \, [\dot{\mathbf{x}}(\tau)]^2 - \frac{a}{2} \int_0^t d\tau \int_0^t d\tau' |\mathbf{x}(\tau) - \mathbf{x}(\tau')|^2 \frac{\cos[b(|\tau - \tau'| - t/2)]}{\sin(bt/2)} \, , \tag{3.9}$$

where

$$K_{\text{trial}} = 4a/b \quad \text{and} \quad M_{\text{trial}} = 4a/b^3 \, . \tag{3.10}$$

Following the procedure outlined in Ref. 15, the first cumulant approximation is

$$\int \mathcal{D}\mathbf{x}(\tau) e^{i\hbar^{-1} S_{\text{eff}}} \sim \left[\frac{m^*}{2\pi i \hbar t} \right]^{3/2} \left[\frac{v \sin(bt/2)}{b \sin(vt/2)} \right]^3 e^{I_0(t) + I_{\text{int}}(t) + I_{\text{dis}}(t)} \, , \tag{3.11a}$$

where $v \equiv [K_{\text{trial}}(m^* + M_{\text{trial}})/m^* M_{\text{trial}}]^{1/2}$ and $b \equiv (K_{\text{trial}}/M_{\text{trial}})^{1/2}$,

$$I_0(t) = \frac{3M_{\text{trial}}}{2(m^* + M_{\text{trial}})} \left[\frac{vt}{2} \cot \left[\frac{vt}{2} \right] - 1 \right] \, , \tag{3.11b}$$

$$I_{\text{int}}(t) = -\frac{\pi}{2} \left[\frac{u}{k_0} \right]^2 \int_0^t d\Delta(t - \Delta) \int_0^\infty dk \, k^3 \exp \left[-\frac{k^2}{2k_0^2} [\pi - iQ(\Delta; t)] \right] \left\{ [N(k) + 1] e^{-iuk\Delta} + N(k) e^{iuk\Delta} \right\} \, , \tag{3.11c}$$

$$I_{\text{dis}}(t) = -\int_0^t d\Delta(t - \Delta) \left[\frac{(k_0 L)^3 V_{\text{rms}}^2}{8\hbar^2} \left[\frac{(k_0 L)^2}{4} - \frac{i}{2} Q(\Delta; t) \right]^{-3/2} \right] \, , \tag{3.11d}$$

$$Q(\Delta; t) = \hbar k_0^2 \left[\frac{2M_{\text{trial}}}{m^*(m^* + M_{\text{trial}})v} \frac{\sin(v\Delta/2)\sin[v(\Delta - t)/2]}{\sin(vt/2)} + \frac{(\Delta - t)\Delta}{(m^* + M_{\text{trial}})t} \right] \, , \tag{3.11e}$$

and $N(k) \equiv (e^{\hbar uk\beta} - 1)^{-1}$.

Expression (3.11a) has poles along the real time axis spaced by $2\pi/v$. It is convenient to shift the time contour in (3.1) into the lower half complex time plane and perform the integration over all real t', with $t = -iT + t'$. For imaginary time $t = -iT$ and $vt \gg 1$, Eqs. (3.11b) and (3.11e) may be approximated by

$$I_0(t) \approx \frac{3M_{\text{trial}}}{4(m^* + M_{\text{trial}})} vit - \frac{3M_{\text{trial}}}{(m^* + M_{\text{trial}})} \, , \tag{3.12a}$$

$$Q(\Delta; t) \approx i\hbar k_0^2 \left[\frac{M_{\text{trial}}}{m^*(m^* + M_{\text{trial}})v} - \frac{i(\Delta - t)\Delta}{t(m^* + M_{\text{trial}})} \right] \, , \tag{3.12b}$$

so,

$$e^{it(v - E_{\text{gap}}/\hbar)} \int \mathcal{D}\mathbf{x}(\tau) e^{i\hbar^{-1} S_{\text{eff}}}$$

$$\approx \left[\frac{m^* + M_{\text{trial}}}{2\pi\hbar t} \right]^{3/2} \sin^3(bt/2) \exp F(t) \, , \tag{3.13a}$$

where

$$F(t) = -\frac{3M_{\text{trial}}}{2(m^* + M_{\text{trial}})}$$

$$+ it \left[v - E_{\text{gap}}/\hbar + \frac{3M_{\text{trial}}v}{4(m^* + M_{\text{trial}})} - 3v/2 \right]$$

$$+ I_{\text{int}}(t) + I_{\text{dis}}(t) \, . \tag{3.13b}$$

In order to make a connection with Toyozawa's expressions for absorption in the adiabatic limit of electron-phonon interaction,[18] one must consider (3.11c)

in the adiabatic limit ($M_{\text{trial}} \to \infty$):

$$I_{\text{int}} \to \frac{\pi}{2} S_{\text{ac}} \frac{1}{k_0^2} \int_0^\infty dk \, k \exp \left[-\frac{k^2}{k_0^2} \left[\frac{\pi}{2} + \frac{\hbar uk_0}{2mv} \right] \right]$$

$$\times \left\{ [N(k) + 1] e^{-iukt} + N(k) e^{iukt} - 2N(k) - 1 \right\} \, . \tag{3.14}$$

Following Toyozawa we define

$$S_\pm \equiv \frac{\pi S_{\text{ac}}}{2k_0^2} \int_0^\infty dk \, k \exp \left[-\frac{k^2}{k_0^2} \left[\frac{\pi}{2} + \frac{\hbar uk_0}{2mv} \right] \right]$$

$$\times \left[\begin{matrix} N(k) + 1 \\ N(k) \end{matrix} \right] \exp(\mp iukt) \, , \tag{3.15a}$$

$$S \equiv S_+(0) + S_-(0)$$

$$= \frac{\pi S_{\text{ac}}}{2k_0^2} \int_0^\infty dk \, k \exp \left[-\frac{k^2}{k_0^2} \left[\frac{\pi}{2} + \frac{\hbar uk_0}{2mv} \right] \right]$$

$$\times [2N(k) + 1] \, . \tag{3.15b}$$

Now $\exp I_{\text{int}}(t) = \exp[S_+(t) + S_-(t) - S]$ can be expanded in a power series of $S\pm(t)$. The zeroth-order term is the zero phonon line, with intensity proportional to $\exp(-S)$. The general term $S_+(t)^{n_+} S_-(t)^{n_-}$ represents the emission of n_+ phonons and the absorption of n_- phonons during the optically induced electronic transition. Emitted phonons cost elastic energy, therefore, the photon energy $h\nu$ must be increased. Thermal fluctuations enhance the phonon emissions, however, they persist down to zero temperature. At zero temperature and in the absence of static disorder these emission processes

alone give rise to polaronic states if the electron-phonon coupling constant S_{ac} is sufficiently large. However, the lattice distortion energy prevents states from existing below the polaron ground-state energy. Static potential wells provide nucleation centers below the polaron threshold, allowing states to have energies below the polaron ground-state energy.[15] On the other hand, phonons absorbed from the heat bath during the electronic transition and emitted into the cloud surrounding the electron allow the electron to dig its own potential well at no cost of lattice distortion energy. Thus, even in the absence of static disorder, at finite temperatures phonon absorption sidebands give rise to an infinite tail of localized states below the conduction-band edge.

Returning to the nonadiabatic expression for the absorption coefficient (3.2), the time contour integral was evaluated in a saddle-point approximation. The function $F(t)$ [Eq. (3.13b)] has a saddle point $t_s = -iT_s$ on the negative imaginary time axis. It follows that the exponential part of the absorption coefficient behaves as

$$\alpha(\nu) \sim \exp F(t_s) \ . \tag{3.16}$$

The variational principle derived in Ref. 15 for the DOS is valid with (3.16), thus the variational parameters v and M_{trial} were chosen to maximize $\ln[\alpha(\nu)]$ for every value of v. The time at the saddle point was found by solving $F'(t_s) = 0$. The optimum values of v, M_{trial}, and t_s were determined numerically.

We first consider crystalline silicon. The Debye energy is $\hbar\omega_0 \equiv \hbar u k_0 \approx 0.054$ eV,[21] the average speed of sound is $u \approx 8400$ m/s (Ref. 22) and the conduction-band average effective mass is $m^* \approx 1.1 m_e$.[23] Thus, $\gamma = \hbar u k_0 / (\hbar^2 k_0^2 / 2m^*) \approx 0.016$. The valence-band defor-

mation potential is $E_d \approx 11.3$ eV (Ref. 24) so $S_{ac} \approx 28.8$. In a pure crystalline sample there is no static disorder so $V_{rms} = 0$. Figure 2 shows the numerically evaluated absorption spectra in the range $T = 150-350$ K. Comprehensive measurements of $\alpha(\nu)$ by Cody et al.[25] at 300 K in c-Si reveal an Urbach slope of $E_0 = 8.5 \pm 1.0$ meV in the vicinity of the indirect edge $1.0 \lesssim \hbar\nu \lesssim 1.1$ eV. Our theory, which contains no free parameters, yields accurate linear exponential behavior with a slope of $E_0 = 8.6$ meV. Although it is not difficult to implement the electron crystal momentum k-selection rule into our continuum model, it has been suppressed here since the electronic wave functions are strongly localized at energies in the Urbach regime. The small effects within the Urbach regime would be best treated by a tight binding model.

Measurements of some of the input parameters of a-Si:H have been made. For convenience, we choose γ to have the same value as in c-Si and the correlation length L for the static random potential to be equal to the lattice constant. S_{ac} and V_{rms} of a-Si:H were then uniquely determined by matching the observed temperature dependence of E_0 with our theoretical model, yielding $V_{rms} \simeq 0.41$ eV and $S_{ac} \simeq 220$. A detailed comparison between our theory and measurements of Tiedje et al.[26] is presented in Fig. 3. The absorption coefficient and the conduction-band tail DOS display linear exponential behavior over more than three decades, in agreement with recent photoelectron spectroscopy measurements.[27] A comparison of the polaronic effective masses and radii be-
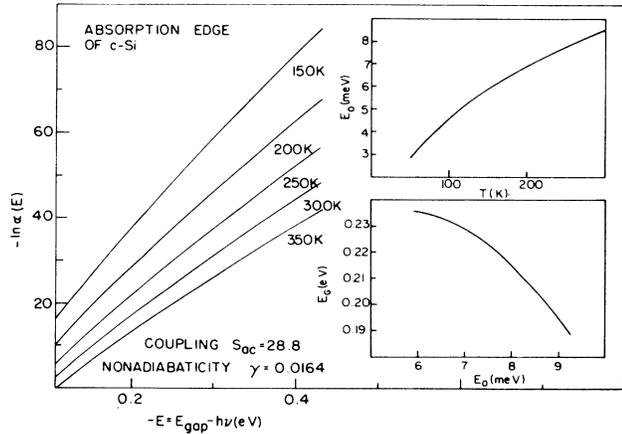

FIG. 2. Absorption coefficient in crystalline silicon (relative to its value at $\hbar\nu = 1.1$ eV for c-Si at 350 K) as a function of energy below the shifted indirect continuum edge at $E \simeq -0.1$ eV for various temperatures. Accurate linear exponential Urbach behavior begins to occur only at $E \simeq -0.3$ eV at 350 K and at the unobservably low energy $E = -0.5$ eV at 150 K. Theoretically it extends at least 0.5 eV below these energies. The upper insert shows E_0 vs temperature. The lower insert contains a plot of the downshift E_G of the continuum edge vs Urbach slope E_0. For high temperatures their relationship becomes linear.
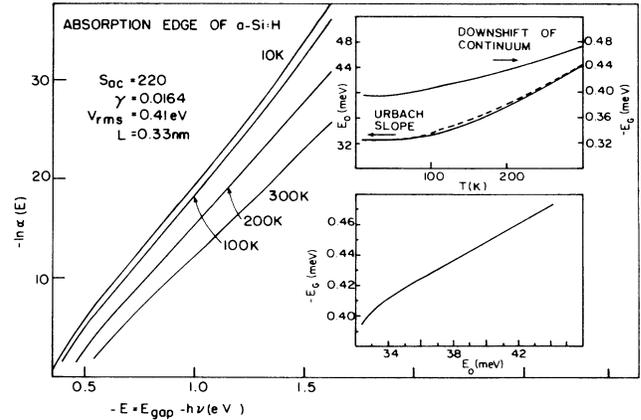

FIG. 3. Absorption coefficient for various temperatures in hydrogenated amorphous silicon. The continuum edge occurs approximately at the left-hand side of each curve. Linear Urbach behavior occurs over energy ranges $-0.6 \gtrsim E \gtrsim -1.1$ eV at 10 K and $-0.8 \gtrsim E \gtrsim -1.3$ eV at 300 K. The Urbach focus is temperature independent. In the upper insert, the solid curve at the bottom is the computed Urbach slope E_0 vs temperature in kelvins for a-Si:H. Superimposed (dashed curve) is the experimentally observed slope (Tiedje et al.). The energy scale for these curves is at the left-hand side of the figure. Also shown is the downshift of the continuum E_G (energy scale on right-hand side of figure). The lower inset shows E_G vs E_0 displaying a linear relationship for $T \gtrsim 100$ K.

tween c-Si and a-Si:H at low and high temperatures is shown in Fig. 4.

Cody first noted a linear relationship between E_0 and E_T, the Tauc energy gap.[19] E_T is determined by fitting $\alpha(\nu)$ at photon energies greater than those in the Urbach regime to the expression

$$[\alpha(\nu)h\nu]^{1/2} = C[h\nu - E_T(T)] . \tag{3.17}$$

The saddle-point approximation made in obtaining (3.16) fails for these photon energies (but is valid in the Urbach regime) so it is difficult to match (3.17) to our theory in order to obtain $E_T(T)$. $E_T(T)$ is commonly used to define the width of the band gap in amorphous semiconductors. Another such measure is $E_G(T)$, the downshift of the continuum band edge associated with the perturbative emission and reabsorption of virtual phonons. E_G is expected to be linearly related to E_T; thus a linear relationship between E_0 and E_G is consistent with experiment.
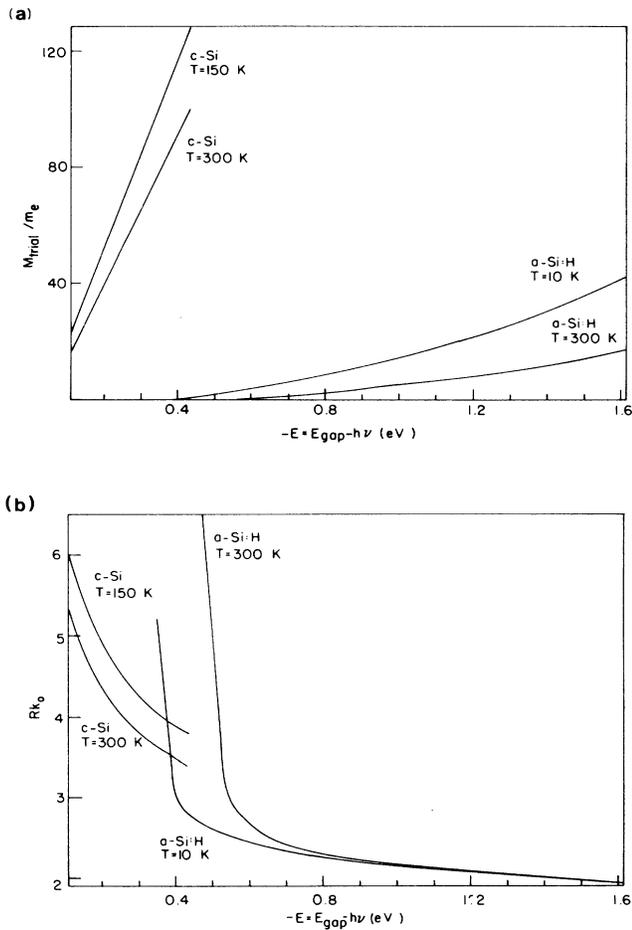

(a)

(b)

FIG. 4. (a) The effective mass of conduction-band-tail states in c-Si and a-Si:H at several temperatures. (b) The polaron radius $Rk_0 \equiv [\hbar k_0^2(m^* + M_{\text{trial}})/m^* M_{\text{trial}}v]^{1/2}$ in the conduction-band tail. k_0 is the Debye wave vector, m^* is the conduction-band electron effective mass, and v measures the electron frequency in its self-trapped state.
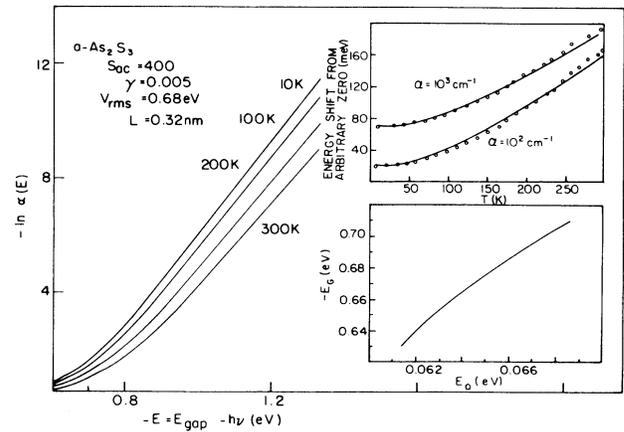
FIG. 5. Absorption coefficient at various temperatures in a-As$_2$S$_3$. The Urbach focus is temperature independent. The upper inset shows the observed photon-energy shift as a function of temperature (points) and the theoretical fit (solid line) at two values of the absorption coefficient. The lower inset shows E_G and E_0 becoming linearly related at high temperatures.

As with a-Si:H, measurements of some of the input parameters of a-As$_2$S$_3$ have not been made. Street et al.[28] estimate the Debye energy to be $\hbar\omega_0 \approx 0.017$ eV. The average speed of sound is $u \approx 2630$ m/s.[29] Assuming $m^* \approx m_e$ yields $\gamma \approx 0.005$. We assume L is approximately equal to the lattice constant. S_{ac} and V_{rms} are determined uniquely by matching the theory to the shifts of photon energies required to give $\alpha = 10^2$ and 10^3 cm^{-1} at various temperatures. These values of the absorption coefficient lie within the Urbach regime. To quantitatively reproduce the data we must choose $E_{\text{gap}} \approx 3.49$ eV and
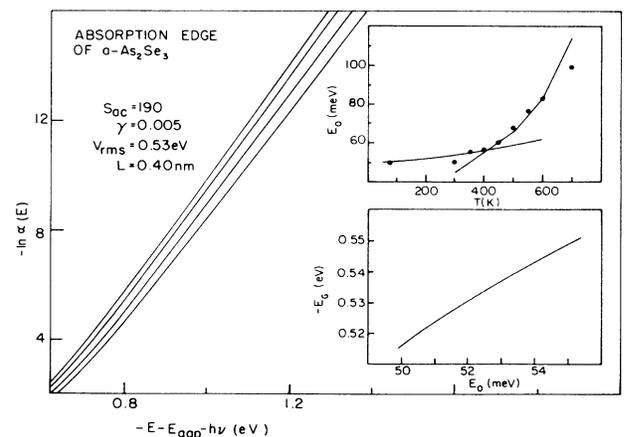
FIG. 6. Absorption coefficient at temperatures 10 (upper curve), 100, 200, and 300 K (lower curve) in a-As$_2$Se$_3$. The Urbach focus is temperature independent. The upper inset shows the observed E_0 vs temperature (points) and the theoretical fits (solid lines) above and below the glass transition temperature $T_g \approx 450$ K. The lower inset shows E_G and E_0 becoming linearly related at high temperatures.

$\alpha_0 \approx 2.3 \times 10^5$ cm^{-1}. This yields $S_{ac} \approx 400$ and $V_{rms} \approx 0.68$ eV. Figure 5 shows a detailed comparison between our theory and Street's results. As with a-Si:H, excellent agreement is found.

Finally, we consider a-As$_2$Se$_3$. The measured input parameters are $\hbar\omega_0 \approx 0.012$ eV and $u \approx 2300$ m/s.[30] Assuming $m \approx m_e$ yields $\gamma \approx 0.005$ as for a-As$_2$S$_3$. Performing the same fit discussed for a-Si:H to match the theory to the temperature dependence of E_0 observed by Andreev et al.[31] yields $S_{ac} \approx 190$ and $V_{rms} \approx 0.53$ eV for temperatures below the glass transition temperature $T_g \approx 450$ K. Although our model is not applicable to liquid semiconductors, we can match the observed temperature dependence of E_0 for $T > T_g$ with $S_{ac} = 1520$, $V_{rms} = 0$, and $\gamma = 0.005$. (Andreev notes that a linear extrapolation of his $T > T_g$ data predicts an Urbach slope $E_0 = 0$ at $T = 0$, thus we choose $V_{rms} = 0$.) This, of course, suggests qualitatively different physics above T_g. A comparison between the theory and Andreev's measurements is shown in Fig. 6.

The crystalline values of S_{ac} have not been experimentally determined for As$_2$Se$_3$ and As$_2$S$_3$, nor have measurements been made of S_{ac} in a-Si:H, a-As$_2$Se$_3$, or a-As$_2$S$_3$. For Si, the large change in S_{ac} from its crystalline value may seem surprising at first. Although for a-Si:H there is some amount of freedom in the choice of γ and hence V_{rms} and S_{ac}, we find that for all choices, the effect of disorder is to move the electron-phonon coupling closer to the small-polaron threshold than in the crystal in order to

obtain a theoretical fit to the experimentally measured $E_0(T)$. This discrepancy is improved somewhat but not substantially by considering the role of the second band tail in determining $\alpha(v)$. We now proceed to discuss the corrections arising from convolving the valence- and conduction-band tails.

IV. COMBINED EFFECTS OF VALENCE- AND CONDUCTION-BAND TAILS

A more refined model involves choosing the initial-state manifold to consist of a set of strongly localized electronic levels with a DOS equal to that of an electron coupled to a phonon field and static random potentials. Our approach here is to mimic both the static and thermal aspects of the disorder in the valence-band tail by means of effective static random potentials. Our treatment is still within a continuum model for the electron dynamics. As a first approximation we again try to mimic some aspects of the true band structure by introducing two independent continua, one for the conduction band and one for the valence band. The computation is greatly simplified by treating the finite temperature phonon field as being frozen in one of the bands. This, nevertheless, gives a good estimate of the magnitude of the correction of the results of Sec. III arising from the presence of two band tails.

The absorption coefficient is proportional to the convolution of the valence- and the conduction-band tail DOS's:

$$\alpha_{total}(v) \sim \mathrm{Av}_i \left\{ \sum_f |R_{i,f}|^2 \delta(E_i + hv - E_f) \right\}$$

$$= \mathrm{Av}_i \left\{ \sum_f |R_{i,f}|^2 \int dE\, \delta(E_i + hv - E)\delta(E - E_f) \right\}$$

$$= \mathrm{Av}_i \left\{ \sum_f |R_{i,f}|^2 \int dE \int_{-\infty}^{\infty} \frac{dt}{2\pi\hbar} \int_{-\infty}^{\infty} \frac{dt'}{2\pi\hbar} e^{it(v + E_i/\hbar - E/\hbar)} e^{it'(E - E_f)/\hbar} \right\} . \tag{4.1}$$

Neglecting the dependence of $R_{i,f}$ on i, f, the total absorption becomes

$$\alpha_{total}(v) \sim \int_{hv - E_{gap}}^{0} dE\, \rho_v(h\tilde{v} - E)\alpha(E) , \tag{4.2}$$

where α is the absorption coefficient calculated in Sec. III. The limits of the E integration have been chosen to limit the initial and final states to subgap states. ρ_v is the valence-band-tail DOS which we approximate by means of two static random potentials, one describing static disorder and one describing a frozen-in phonon distribution. As is discussed in the next section, at high temperatures the electron-acoustic phonon interaction is equivalent to electron-static Gaussian correlated random potential interaction with $V_{rms}^2 = S_{ac} k_B T \hbar\omega_0/\sqrt{2}$ and $L = \sqrt{2\pi}/k_0$. Techniques to calculate ρ_v are presented in Ref. 15, they are similar to those used in this paper. Considering the convolution of the dominant Urbach regimes of ρ_v and α, then letting

$$\rho_v(E) = e^{(E - E_{gap})/E_V} , \tag{4.3a}$$

$$\alpha(E) = e^{E/E_c} \tag{4.3b}$$

one obtains

$$\alpha_{total}(v) \sim \frac{E_C E_V}{E_V - E_C}\left(e^{(hv - E_{gap})/E_V} - e^{(hv - E_{gap})/E_C} \right) . \tag{4.4}$$

Thus, if either E_V or E_C is much larger than the other, absorption is dominated by the band tail with the larger Urbach slope. If the valence- and conduction-band-tail Urbach slopes are comparable, say $E_V = E_0 + \Delta$ and $E_C = E_0 - \Delta$, then α_{total} behaves as a single linear exponential with Urbach slope E_0 in the limit $\Delta \to 0$. In neither of these cases does the presence of a second band tail with smaller or comparable Urbach slope significantly alter the absorption coefficient calculated for a single band tail as in Sec. III.

For the case of a-Si:H, employing the above method to calculate α_{total} yields a fit to the data of Tiedje et al. with

$S_{ac} \approx 200$ in both of the band tails. This value of S_{ac} in the conduction-band tail is slightly less than that obtained in the earlier approximation of a single level in the initial-state manifold but is still greater than the observed value in c-Si.

A proper treatment of the electron dynamics in the valence-band tail and the inclusion of correlation effects between the valence- and the conduction-band tails may yield a further decrease in the values of S_{ac} needed to fit the experimental data. Moreover, our models assume a linear dispersion relation for acoustic phonons. This is a poor approximation in amorphous materials.[32, 33] The consideration of a more appropriate acoustic-phonon dispersion relationship and the presence of localized phonon modes may enhance the effective S_{ac} in the amorphous material.

V. MOST-PROBABLE–POTENTIAL-WELL METHOD

A simple physical argument[8, 16] may be used to obtain the zero-temperature DOS of a coupled electron-phonon system in the presence of static disorder, in the adiabatic limit.[15] In this section a similar method is used to calculate an approximation to the exponential part of the finite-temperature absorption coefficient.

Consider the quantum mechanical probability distribution for normal coordinates q_k of a lattice at finite temperature:

$$P_1\{q_k\} \propto \prod_k \sum_{n_k} |\phi_{n_k}(q_k)|^2 e^{-\beta(n_k + 1/2)\hbar\omega_k}$$

$$\sim \exp \sum_k \left[-\frac{M\omega_k q_k^2}{\hbar \sinh(\hbar\omega_k\beta)} \right.$$

$$\left. \times [\cosh(\hbar\omega_k\beta) - 1] \right], \quad (5.1)$$

where the ϕ_{n_k} are harmonic oscillator wave functions and the product is over all wave vectors k in the first Brillouin zone. We consider lattice fluctuations of the form

$$q_k = \frac{iQ_0}{\sqrt{N}} \exp \left[-\frac{k^2 c^2}{4} \right], \quad (5.2)$$

of depth Q_0, and range c. In order to make contact with the continuum theory, it is convenient to replace the wave-vector summation in (5.1) by an integral:

$$\sum_k \rightarrow \frac{V}{(2\pi)^3} \int d^3k \, C^{-1}(k) \quad (5.3)$$

with autocorrelation function $C(k)$ chosen to have a Gaussian form, with correlation length $\sqrt{2\pi}/k_0$ (Ref. 15),

$$C(k) = \exp \left[-\frac{\pi k^2}{2k_0^2} \right]. \quad (5.4)$$

The probability of occurrence of a fluctuation of the form (5.2) is given by

$$P_1\{q_k\} \propto \exp \left[- \left[\frac{\pi}{4k_0^4} \right] \frac{\hbar u k_0}{(\hbar^2/2MQ_0^2)} \right.$$

$$\times \int_0^\infty dk \, k^3 e^{-k^2(c^2 - \pi/k_0^2)/2}$$

$$\left. \times \frac{\cosh(\hbar u k\beta) - 1}{\sinh(\hbar u k\beta)} \right]. \quad (5.5)$$

In addition to the probability distribution of dynamic lattice fluctuations due to phonons the probability distribution fixed potentials due to static disorder must also be considered. The Fourier components of a correlated Gaussian random potential obey the probability distribution[15]

$$P_2\{V(k)\} \propto \exp \left[-\frac{1}{2} \int \frac{d^3k}{(2\pi)^3} V(k) B^{-1}(k) V(-k) \right] \quad (5.6)$$

with autocorrelation function chosen to be

$$B(k) = V_{rms}^2 (\pi L^2)^{3/2} \exp \left[-\frac{k^2 L^2}{4} \right], \quad (5.7)$$

and correlation length L [(5.7) is equivalent to (3.8)]. We consider static potential wells of Gaussian form characterized by a depth V_0 and range A:

$$V(r) = -V_0 \exp \left[-\frac{r^2}{A^2} \right], \quad (5.8)$$

so (5.6) becomes

$$P_2\{V(k)\} \propto \exp \left[-\frac{V_0^2}{2V_{rms}^2} \left[\frac{1}{Z} \right]^{3/2} (2-Z)^{-3/2} \right], \quad (5.9)$$

where $Z \equiv (L/A)^2$.

Thus, the joint probability distribution of fluctuations (5.2) and (5.8) is

$$P\{V(k), q_k\} \propto P_1\{q_k\} P_2\{V(k)\}. \quad (5.10)$$

The variational parameters Z, V_0, Q_0, and c are constrained by the radial Schrödinger equation to provide a ground state at energy E

$$\left[-\frac{\hbar^2}{2m^*} \frac{d^2}{dr^2} - V_0 e^{-r^2/A^2} + \frac{E_d}{u} \sum_k \dot{q}_k \frac{e^{ik \cdot r}}{\sqrt{N}} \right] u(r)$$

$$= -|E| u(r), \quad (5.11)$$

where $u(r) \equiv r\psi(r)$ and $\psi(r)$ is the electronic wave function. Equation (5.11) contains two potential terms: the static Gaussian potential and the deformation potential describing interaction between the electron and acoustic phonons. The variational parameters are chosen to maximize (5.10) subject to constraint (5.11).

With this choice of the variational parameters, (5.10) becomes an estimate of the one-electron DOS in a single band tail. Absorption coefficient (3.16) is essentially the DOS in the conduction-band tail with the added contributions of phonon sidebands. To approximate the effects of phonon sidebands, the lattice distortion energy was not included in (5.11). Thus, the phonon contribution to

(5.10) will be similar to the static disorder contribution, that is, an infinite tail forms rather than a tail which vanishes at the polaron ground-state energy in the absence of static disorder. Note that in the limit of high temperature ($\beta \rightarrow 0$) the phonon probability distribution (5.5) becomes equivalent to the static disorder distribution (5.9). Similarly, for the path integral, in the adiabatic ($M_{\text{trial}} \rightarrow \infty$) and small-time $[uk_0 T_s/(\pi/2 + \hbar uk_0^2/2mv) \ll 1]$ limits, the phonon contribution (3.11c) to the absorption coefficient in the saddle-point approximation becomes equivalent to the static-disorder contribution (3.11d). A numerical comparison between (3.16) and (5.10) in the above limits with $V_{\text{rms}} = 0$ reveals that the most-probable–potential-well method does not include the correct phonon emission amplitude. The two methods agree when the phonon emission term $[N(k)+1]e^{-iuk\Delta}$ in (3.11c) is modified to $e^{-iuk\Delta}$. Figure 7 presents a comparison between the predictions of the most-probable–potential-well method and the path-integral method with and without the modification to the phonon emission term. The absorption coefficient predicted by the most-probable–potential-well method is slightly greater than that obtained from the modified path-integral method for all energies because the former method does not restrict the wave function to a particular form whereas the latter method restricts the wave function to a harmonic-oscillator form.

It is apparent that our multiple phonon emission and absorption sideband model goes beyond the static potential-well picture in several important ways. First of all, it correctly incorporates the dynamics of the potential wells arising from the nonadiabaticity of the electron-phonon interaction. By doing so, our model recovers the usual small polaron theory in the limit of zero tempera-
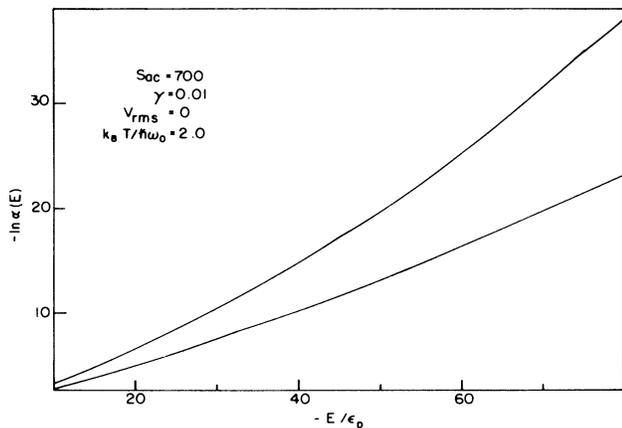
ture. At zero temperature there is a lower bound to the absorption edge given by the ground state of the coupled electron-phonon system. As the temperature is turned on, an infinite absorption tail immediately emerges since phonons can be absorbed from the heat bath and reemitted into a polaronic potential well. In the static potential-well picture this emission process requires elastic deformation energy. However, this elastic energy is now provided by the heat bath. That is to say, the simple physical arguments of this section with the inclusion of elastic energy can recover the path-integral theory if the phonon absorption term is removed and the phonon emission amplitude $N(k)+1$ is replaced by 1. If the phonon absorption term is included in the path integral and the emission amplitude is kept at unity the potential-well calculation must be performed without including elastic deformation energy. The fact that the potential-well picture does not capture the full physics of the path integral is because the potential-well technique is basically an effective DOS, whereas, the true optical transition amplitude involves an enumeration of all possible processes which can couple the electron from the valence band to such an effective DOS. In particular the phonon emission amplitude at finite temperature is modified by the usual Bose factor $N(k)+1$. Such a modification does not appear in the potential-well method.

VI. DISCUSSION AND SUMMARY

The simple model of a strongly localized initial state and a more complete treatment of the electron-phonon and electron–static-disorder interaction in the final state yields an excellent fit to the observed temperature dependence of the Urbach slope E_0 and the downshift of the continuum E_G and the temperature independence of the Urbach focus in the materials c-Si, a-Si:H, a-As$_2$Se$_3$, and a-As$_2$S$_3$. Phonon sidebands in the absorption spectra arise from the nonlinear electron-phonon interaction and account for most of the observed features of the absorption spectra in the Urbach regime.

At high temperatures the electron-phonon interaction becomes equivalent to electron-Gaussian correlated random potential interaction with an effective temperature-dependent disorder strength V_{rms}. For a Gaussian correlated random potential it has been shown that $E_G \propto V_{\text{rms}}^2$,[34] and $E_0 \propto V_{\text{rms}}^2$.[8] Thus, E_0 and E_G are expected to be linearly related at high temperatures as is verified by our theory and experiments. At low temperatures our theory predicts departures from linearity characteristic of the quantum nature of the lattice vibrations.

Our model is valid in materials in which the exciton binding energy is small compared with the energy scale of the disorder, resulting in the exciton line occurring at energies higher than those in the Urbach regime. Electron-hole correlations are of great importance in certain polar semiconductors or ionic insulators where disorder may cause field ionized exciton states,[35] causing an associated dependence in the dipole matrix element.

The observed linearity of Urbach tails is a consequence of short-range order in both thermally disordered and

FIG. 7. A comparison of the most-probable–potential-well method and the path-integral method to calculate the absorption coefficient. $\epsilon_D \equiv \hbar \omega_0$ is the Debye energy. The low curve is calculated by means of path integrals in the adiabatic limit of electron-phonon interaction. The upper curve is obtained by means of the most-probable–potential-well method and coincides with the path-integral method if the phonon emission amplitude $[N(\omega_k)+1]$ is replaced by unity in the path-integral method.

amorphous materials. For Gaussian correlated random potentials, the correlation length must be close to the lattice spacing. For phonons in our continuum model, short-range order is determined by the high-frequency cutoff. Linear Urbach behavior survives the combination of static disorder and dynamic electron-phonon interactions.

This work develops an explanation of some of the main features of Urbach tails in certain materials. A complete theory requires the incorporation of exciton effects, real band structure, and a more complete treatment of the dynamics of electrons and holes in the valence-band tail.

ACKNOWLEDGMENTS

APPENDIX

This appendix outlines the evaluation of the path integrals over the phonon coordinates and the integrals over the end points q_k and q'_k in the expression

$$\int \prod_k (dq_k \, dq'_k) \langle \{q_k\} | e^{-(\beta - it/\hbar)H_{ac}} | \{q'_k\} \rangle$$

$$\times \langle 0; \{q'_k\} | e^{-iHt/\hbar} | 0; \{q_k\} \rangle \ . \quad \text{(A1)}$$

Consider

$$\langle 0; \{q'_k\} | e^{-iHt/\hbar} | 0; \{q_k\} \rangle = \int \mathcal{D}\mathbf{x}(\tau) \mathcal{D}q \, \mathbf{k}(\tau) e^{iS/\hbar} \ , \quad \text{(A2a)}$$

where

$$S = S_e + S_{e\text{-ac}} + S_{\text{dis}} \ , \quad \text{(A2b)}$$

$$S_e = \frac{m^*}{2} \int_0^t d\tau \, \mathbf{x}^2(\tau) \ , \quad \text{(A2c)}$$

$$S_{e-\text{ac}} = \int_0^t d\tau \frac{M}{2}(|\dot{q}_k|^2 - \omega_k^2 |q_k|^2) + \gamma_k(\tau)\dot{q}_k(\tau) \ , \quad \text{(A2d)}$$

$$S_{\text{dis}} = -\int_0^t d\tau \sum_{j=1}^{N_d} v(\mathbf{x}(\tau) - \mathbf{R}_j) \ , \quad \text{(A2e)}$$

and

$$\gamma_k(\tau) = \frac{E_d}{u} \frac{e^{i\mathbf{k}\cdot\mathbf{x}}}{\sqrt{N}} \ . \quad \text{(A2f)}$$

To facilitate the evaluation of the phonon path integrals, let

$$I_k(\gamma) \equiv \int \mathcal{D}q_k \mathcal{D}q_{-k} e^{i(S_k + S_{-k})/\hbar} \quad \text{(A3a)}$$

where

$$S_k = \frac{M}{2} \int_0^t d\tau (|\dot{q}_k|^2 - \omega_k^2 |q_k|^2) + \int_0^t \gamma_{\hbar}(\tau)\dot{q}_{\hbar}(\tau) \ . \quad \text{(A3b)}$$

Letting $q_k = u_k + i v_k$ and $\gamma_k = \gamma_k^r + i\gamma_k^i$ yields

$$I_k(\gamma) = I_k^u(\gamma) I_k^v(\gamma) \ , \quad \text{(A4a)}$$

where

$$I_k^u(\gamma) = \int_{u_k(0)=u_k, \, u_k(t)=u'_k} \mathcal{D}u_k \exp\left[i\left[S_0(u_k) - 2\int_0^t d\tau \, u_k \dot{\gamma}_k^r\right]/\hbar\right] \ , \quad \text{(A4b)}$$

$$I_k^v(\gamma) = \int_{v_k(0)=v_k, \, v_k(t)=v'_k} \mathcal{D}v_k \exp\left[i\left[S_0(v_k) + 2\int_0^t d\tau \, v_k \dot{\gamma}_k^i\right]/\hbar\right] \ , \quad \text{(A4c)}$$

and

$$S_0(x) = M \int_0^t d\tau (\dot{x}^2 - \omega_k^2 x^2) \ . \quad \text{(A4d)}$$

Noting that the action in (A4b) is that of a driven harmonic oscillator, one obtains from Feynman and Hibbs[10]

$$I_k^u(\gamma) = \left[\frac{M\omega_k}{\pi i\hbar \sin(\omega_k t)}\right]^{1/2} e^{iS_{cl}^u/\hbar} \ , \quad \text{(A5a)}$$

where

$$S_{cl}^u = \frac{M\omega_k}{\sin(\omega_k t)}\left[\cos(\omega_k t)(u_k^2 + u'^2_k) - 2u_k u'_k - \frac{2u_k}{M\omega_k}\int_0^t d\tau \, \dot{\gamma}_k^r(\tau)\sin[\omega_k(t-\tau)] - \frac{2u'_k}{M\omega_k}\int_0^t d\tau \, \dot{\gamma}_k^r(\tau)\sin(\omega_k \tau)\right.$$

$$\left. - \frac{2}{M^2\omega_k^2}\int_0^t d\tau \int_0^\tau d\tau' \dot{\gamma}_k^r(\tau)\dot{\gamma}_k^r(\tau')\sin[\omega_k(t-\tau)]\sin(\omega_k \tau')\right] \quad \text{(A5b)}$$

and similarly for $I_k^v(\gamma)$.

Also, defining $\langle \{q_k\} | e^{-(\beta - it/\hbar)H_{ac}} | \{q'_k\} \rangle \equiv \int \mathcal{D}q_k(\tau) e^{iS'_k}$ and $J_k^u J_k^v \equiv \int \mathcal{D}q_k \mathcal{D}q_{-k} e^{i(S'_k + S'_{-k})/\hbar}$, then, from Feynman and Hibbs,

$$J_k^u = \left[\frac{M\omega_k}{\pi\hbar \sin[\omega_k(\hbar\beta - it)]}\right]^{1/2} \exp\left[-\frac{M\omega_k}{\hbar \sinh[\omega_k(\hbar\beta - it)]}\{(u_k^2 + u'^2_k)\cosh[\omega_k(\hbar\beta - it)] - 2u_k u'_k\}\right] \quad \text{(A6)}$$

and similarly for J_k^v.

It then follows that (A1) equals

$$\int \mathscr{D}x(\tau) \prod_{k,k_1>0} \left[\int_{-\infty}^{\infty} du_k \int_{-\infty}^{\infty} du'_k I_k^u J_k^u \right] \left[\int_{-\infty}^{\infty} dv_k \int_{-\infty}^{\infty} dv'_k I_k^v J_k^v \right] e^{i(S_e+S_{dis})/\hbar} = \int_{x(0)=x(t)=0} \mathscr{D}x(\tau) e^{iS_{eff}/\hbar}$$

with S_{eff} given by (3.5).

[1]F. Urbach, Phys. Rev. **92**, 1324 (1953); W. Martienssen, J. Phys. Chem. Solids **2**, 257 (1957).

[2]I. M. Lifshitz, Zh. Eksp. Teor. Fiz. **44**, 1723 (1963) [Sov. Phys.—JETP **17**, 1159 (1963)].

[3]E. O. Kane, Phys. Rev. **131**, 79 (1963).

[4]B. I. Halperin and M. Lax, Phys. Rev. **148**, 722 (1966).

[5]J. L. Cardy, J. Phys. C **11**, L321 (1978).

[6]S. John and M. J. Stephen, J. Phys. C **17**, L559 (1984).

[7]W. Sritrakool, V. Sa-yakanit, and H. R. Glyde, Phys. Rev. B **33**, 1199 (1986).

[8]S. John, C. Soukoulis, M. H. Cohen, and E. Economou, Phys. Rev. Lett. **57**, 1777 (1986).

[9]L. Landau, Phys. Sowjet. **3**, 664 (1933).

[10]R. P. Feynman, Phys. Rev. **97**, 660 (1955); R. P. Feynman and A. R. Hibbs, *Quantum Mechanics and Path Integrals* (McGraw-Hill, New York, 1965).

[11]Y. Toyozawa, Prog. Theor. Phys. **26**, 29 (1961).

[12]A. Sumi and Y. Toyozawa, J. Phys. Soc. Jpn. **55**, 137 (1973).

[13]D. Emin and T. Holstein, Phys. Rev. Lett. **36**, 323 (1976).

[14]S. John and M. H. Cohen, Phys. Rev. B **34**, 2428 (1986).

[15]C. H. Grein and S. John, Phys. Rev. B **36**, 7457 (1987).

[16]S. John, Phys. Rev. B **35**, 9291 (1987).

[17]C. H. Grein and Sajeev John (unpublished).

[18]S. Nakajima, Y. Toyozawa, and R. Abe, *The Physics of Elementary Excitations* (Springer-Verlag, Berlin, 1980).

[19]G. D. Cody in *Semiconductors and Semimetals*, edited by J. I. Pankove (Academic, New York, 1984), Vol. 21B, Chap. 2.

[20]V. Samanthyakanit, J. Phys. C **7**, 2849 (1974).

[21]C. Kittel, *Introduction to Solid State Physics* (Wiley, New York, 1976).

[22]W. Senn, G. Winterling, M. Grimsditch, and M. Brodsky, in *Physics of Semiconductors*, edited by B. L. H. Wilson (IOP, Bristol, 1978), p. 709.

[23]*AIP Handbook*, edited by D. E. Gray (McGraw-Hill, New York, 1972), pp. 9–58.

[24]J. Bardeen and W. Shockley, Phys. Rev. **80**, 72 (1950).

[25]G. D. Cody and B. G. Brooks (private communication).

[26]T. Tiedje and J. M. Cebulka, Phys. Rev. B **28**, 7075 (1983).

[27]K. Winer, I. Hirabayashi, and L. Ley, Phys. Rev. Lett. **60**, 2697 (1988).

[28]R. A. Street, T. M. Searle, I. G. Austin, and R. S. Sussmann, J. Phys. C **7**, 1582 (1974).

[29]R. J. Nemanich, Phys. Rev. B **16**, 1655 (1977).

[30]T. N. Claytor and R. J. Sladek, Phys. Rev. B **18**, 5842 (1978).

[31]A. A. Andreev, B. T. Kolomiets, T. F. Mazets, A. L. Manukyon, and S. K. Pavlov, Fiz. Tverd. Tela (Leningrad) **18**, 53 (1976) [Sov. Phys.—Solid State **18**, 29 (1976)].

[32]R. Biswas, A. M. Bouchard, W. A. Kamitakahara, G. S. Grest, and C. M. Soukoulis, Phys. Rev. Lett. **60**, 2280 (1988).

[33]R. Car and M. Parrinello, Phys. Rev. Lett. **60**, 204 (1988).

[34]S. John, M. Y. Chou, M. H. Cohen, and C. M. Soukoulis, Phys. Rev. B **37**, 6963 (1988).

[35]J. D. Dow and D. Redfield, Phys. Rev B **5**, 594 (1971).